

Manuscript refereed by Dr Mark Dougan (AMES SA, Spain)

Metal Powder/Fly Ash Cenosphere/Modified Clay, Composite

A. Shishkin^{1-a}, V. Mironovs^{1-b}, V. Zemchenkov^{1-c}, I. Hussainova^{2-d}

¹Riga Technical University, Laboratory of Powder Materials, Āzenes Street 16/20, lab. 331, LV – 1048, Riga, Latvia.

²Tallinn University of Technology, Faculty of Mechanical Engineering: Department of Materials Engineering, Ehitajate tee 5, room VI 409, 19086 Tallinn, Estonia,

^apowder.al.b@gmail.com, ^bviktors.mironovs@rtu.lv, ^cv.zemchenkov@gmail.com

^dirina.hussainova@ttu.ee

Abstract

Lightweight structures are a modern trend in material design. The drive and control systems in mechanical engineering require lightweight design provided by the recently developed light materials. Present paper describes metal powder (Fe)/fly ash ceramic cenosphere (CS)/clay ceramic composite material (CM) design and characterisation. Properties of raw material (CS) such as bulk density; phases transition during thermal treatment established by XRD, morphology by SEM; and chemical composition of used clay by gravimetric method are described. Such characteristics as compressive strength, water uptake, and friction coefficient of obtained Fe/CS CM are determined. Dependence of compressive strength from firing temperature, with maximum at 344.00MPa is established. Obtained Fe/CS CM are proposed as a potential anti-friction material.

Keywords: cenosphere, alumina-silica hollow microsphere, lightweight cermet, composite material, friction coefficient, wear

INTRODUCTION

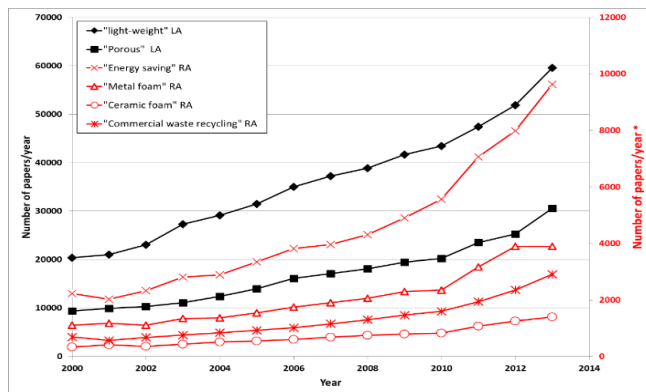


Figure 1. Statistical data from Science Direct web directory (12.06.2014)

plasticity, alumina-silica hollow spheres – fly ash cenospheres (CS) as wear-resistant component and as the same time space holder and modified natural clay (Cl) as inorganic binder between CS and Fe particles were selected.

The advantages of using CS as the carrier are their sphericity, non-toxicity, low weight, and high strength, making them ideal for incorporation into materials such as silicone rubber in order to decrease the thermal conductivity. Furthermore, this enhances rubber's suitability for use as electromagnetic wave absorbing material, which can be used for electronic and radar applications [2]. The lightweight nature of the CS renders them suitable for the design of lightweight composite materials. A variety of different composites have been evaluated, such as CS incorporated into ceramics and concrete [3]–[10], polymers and resins [11]–[15], metals and alloys [16]–[19].

The design of lightweight (porous or cellular structures), cheap but durable materials is one of the modern trends in material design [1].

Problems of recycling and reuse of post-industrial wastes and energy saving became very significant last decade. The following diagram summarizes statistical data regarding number of publication selected by the following keywords in the title: *Light-weight, Porous, Energy saving, Metal foam, Ceramic foam, Commercial waste recycling* Fig 1. The presented trends require new smart approaches in materials design.

For the design of the new material fine iron powder (Fe) as matrix with

Our previous research [20] demonstrates potential for developing of light-weight materials using CS. Obtained first prototypes of material demonstrate compression strength 150-350 Mpa. Taking into account properties of components used in that material design, one of the possible avenues of its application is friction material with reduced weight.

There are numerous ways to produce porous materials. The following techniques are usually chosen in the case of porous metals and alloys: in-situ gas raising, direct foaming, stir casting, sacrificial templates, powder metallurgy, etc. One of the widely used method for obtaining metal syntactic foams is stir casting, using hollow constituents (especially hollow micro spheres [21], or CS [6], [19])

A group of investigators made attempts to synthesize CS filled syntactic foam (SF) for application in structural components like sandwich cores, fire proof and sound damping panels, energy absorbing packaging, underwater buoyant structures etc. [14–17]. These can also be used for electromagnetic shielding of electronic instruments/components and housing of sophisticated equipment. Mostly attempts were made to synthesize CS filled syntactic aluminum foam by melt infiltration [14–18]. However, this method has the limitation of infiltration thickness and thus only small sized samples of SF could be prepared by this technique. The problem in mixing these CS through stirring, and holding the dispersed CS in the melt for sufficient duration because of their very low density as compared to the alloy melt, arises. Another problem is a the melting temperature of the metal or alloy; for aluminum and magnesium it is below 800C, but for such metals and their alloys as iron, copper, nickel, titanium it will be significantly higher than 1000C. For syntactic foams made from these materials a powder metallurgy route is used, where hollow filler is mixed with metal powder before shaping (compaction) and sintering. This technique is widely used for titanium SF [22].

In this study a composite material with the significantly increased density was produced by filling with CS. Modified natural clay was used for the improved binding of iron particles and CS. A closed cell composite foam of uniform cell size and distribution was obtained. Microstructural, mechanical, and physical properties of the new composite foam were studied using various techniques, including optical microscopy, scanning electron microscopy (SEM), energy dispersive X-ray spectroscopy (EDS), and monotonic compression tests.

2. EXPERIMENTAL

2.1. Microstructural characterization, thermal treatment, compression test.

A Scanning Electron Microscope (SEM) Zeiss EVO MA-15, with backscattered electrons (BSE) and secondary electrons modes (SE) was used. Black and white (B&W) images were made in computer. B&W images were analyzed in Image Pro 7, image analysis system (Media Cybernetics). EDS equipped with INCA Energy 350 was used to evaluate CS morphology and structure. The cryogenic fracture surface was used to take scanning electron micrograph. Keyence corporation VHX-2000 optical microscope with lenses VH-Z20R/W and VH-Z500R/W was used for optical imaging.

XRD measurements were performed using Rigaku Ultima+ diffractometer with Cu K α irradiation ($\lambda = 1.541836 \text{ \AA}$) in $2\theta/\theta$ -scanning mode at 2° min^{-1} in steps of 0.02° . Identification of the crystalline phases was carried out with the help of International Centre for Diffraction Data (ICDD) database and SLeve+2008 software.

For firing samples NABERTHERM Laboratory Furnace L9/13 with controller P330 was used. For each sample the mechanical properties, including density, open porosity and compression test, were determined. The density and open porosity was measured by the Archimedes method using isopropanol as medium. The Compression tests of sintered cylindrical pallet (15mm dia and 15 mm height) were carried out using Universal Testing Machine (UTM) (Instron: 8801) at room temperature, strain rate 0.01/s. The tests were carried out for a set of five samples in each category.

2.2 Cenosphere properties

The CS from Coal field “Kuznetsky”, combined heat and power plant “Troitskaya” (Russia), provided by “Biotecha Latvia” LTD, were used as space holder in this research. Main characteristics (but not all of them) such as chemical composition, granulometry, morphology, intact/crushed CS ratio were specified by the supplier. Nevertheless it was necessary to determine them precisely since conditions of coal burning and obtaining of CS from fly ash can differ due to seasonal and other factors.

2.2.1 Chemical composition

Chemical composition was determined by the gravimetric method shown in Table 1.

Table 1. Chemical composition of CS

	Composition							Mass loss	
	SiO ₂	Al ₂ O ₃	Fe ₂ O ₃	CaO	MgO	Na ₂ O	K ₂ O	20-400 C°	400-1000 C°
Mass, %	53.8	40.7	1	1.4	0.6	0.5	0.4	0.6	0.4
Accuracy ±, %	0.5	0.7	0.2	0.2	0.2	0.1	0.1	0.1	0.1

2.2.2 Granulometry and bulk density

Grading composition was determined by sieve analysis according to standard DIN 1045–2 am using Retch Vibratory Sieve Shaker AS 200 digit” device equipped with sieves with dimensions according to standard EN 993-2. The grading composition is (mass %) <63µm – 1.70%, 63-75µm – 3.86%, 75-150 – 94.30%, 150-300µm – 0.00%, 600-1180µm – 0.06%, >1180µm – 0.00%

Bulk density was determined with Scott volumeter according to the ISO 3923-2-81 in 6 parallel measurements and was found to be 0.38±0.0013 g/cm³.

2.2.3 Intact/crushed CS ratio determination.

Sample of analysis of 100.00 g CS, 600.0 ml of distilled water and 1.00 of surfactant were mixed in beaker. The mixture was stirred for 10 minutes by use of propeller type mixer with electric drive, with speed at 800 rpm and left for 30 minutes to segregate. The floating fraction was transferred into Büchner funnel and rinsed with distilled water (200 ml) and ethanol (150 ml) to wash off surfactant. Rinsed CS was dried for 1 hour in drying enclosure at temperature of 120°C and weighed. The liquid remaining above the sediments after settling was carefully decanted and sediments were transferred into Büchner funnel, rinsed with distilled water, ethanol, dried for 3 hours at 120°C and weighed. In the course of analysis of CS, it was noticed that after the settling (segregation in floating and non-floating fraction) liquid turned black. After its filtration black sediments remain on the filter. The analysis of sediment was not carried out, but supposedly it consists of coal particles, which are not burned. It was found that that raw CS contain 11.64±0.8% of crushed CS.

2.3 Clay properties

The homogenized Devonian clay from the Liepa deposit (district of Cesis, Latvia), supplier A/S Lode, was used as inorganic binder. The chemical composition has been determined by gravimetric method shown in Table 2.

Table 2. Chemical composition of Liepa clay.

	Composition								Mass loss	
	SiO ₂	Al ₂ O ₃	Fe ₂ O ₃	CaO	MgO	Na ₂ O	K ₂ O	TiO ₂	20-400 C° (-H ₂ O)	400-1000 C° (-CO ₂)
Mass, %	71.22	14.58	4.17	0.37	0.96	0.058	3.21	0.65	0.6	0.4
Accuracy ±, %	0.5	0.7	0.2	0.2	0.2	0.01	0.1	0.1	0.1	0.1

2.4. Iron metal powder

Air filter dust (Höganäs AB, CMS brand) was used as a source of iron powder. The product has high iron content (guaranteed over 90%), and its sieve analysis is <45, µm - 56.8%; 45<212, µm - 43.2%; >212, µm - 0.0%.

2.5 Materials Synthesis

In this study, semi-dry pressing formation method was selected for samples preparation using the following workflow: weighed dry raw materials (clay, iron powder and CS) were placed in plastic container with lid in such amount, that volume of the dry mixture does not exceed 1/3 of the entire volume of the container, and then mixed for 60 seconds at 30 rpm. 10% solution of NaOH (purity 99,9%, *Sigma-Aldrich*) was added to dry mass mixed manually to get homogenous mass. Samples were pressed in 22.5 mm cylindrical templates (200 bar, 120 s) and then dried on gypsum plate in air up to constant mass (3-4

days). Afterwards samples were sintered in non-oxidizing atmosphere (CO/CO₂ gas mixture) at 5 C°/min heating rate for 60 min. Mass of one sample – 15.0 g.

3. RESULTS AND DISCUSSION

3.1. Raw material and synthesized material microstructure

The CS were used without any preliminary preparation. They have uniform spherical shape, are not agglomerated, and have some inclusions. CS surface is smooth, with small cavities (diameter 0.5-1 μm) and bulges (height 3-30 μm) (Fig. 2a, 2b). CS walls have closed porosity, with thickness 2-20μm(Fig. 2c).

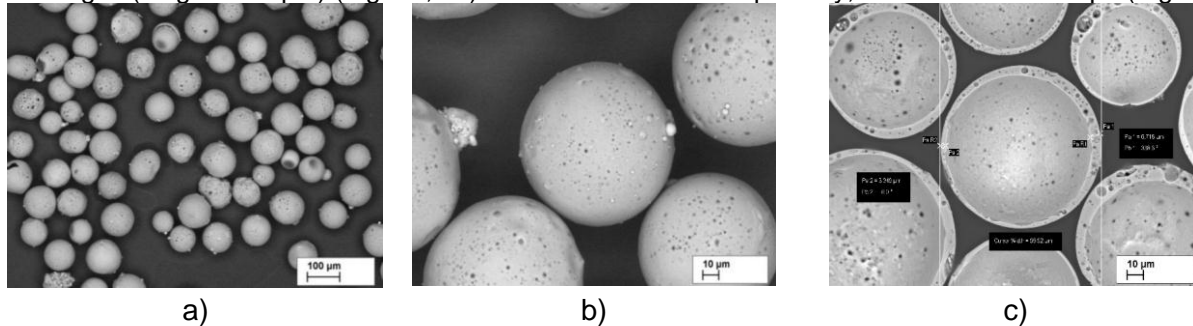


Figure 2 SEM images of CS with magnification 100x (a), 500x (b), cross section at magnification 500x (c)

Metal and non-metal (clay ceramics, CS) particles are uniformly distributed, metal particles have interconnections in all volume of material, forming skeleton (Fig. 3a). The wetting and interfacial bonding between the particle and the matrix appear to be good. CS are also distributed evenly in material volume and are located only in clay ceramic matrix, forming closed porosity (Fig 3b). After analysis of numerous SEM and optical images we concluded that there are no channels but test for open porosity (by water uptake) and picnometric density determination should be performed in the future works for determination of open/close porosity ratio. As well it is necessary to point out good penetration of non-metal phase, mostly clay ceramic, into metal dendritic particles (Fig. 3c, 4a). This is proven by EDX analysis data (Table 3): points 1,2,7 have Si/Al ratio corresponding to clay, 3 and 4 relate to SiO₂ (probably quartz sand grain), 5 and 6 relate to iron powder particles.

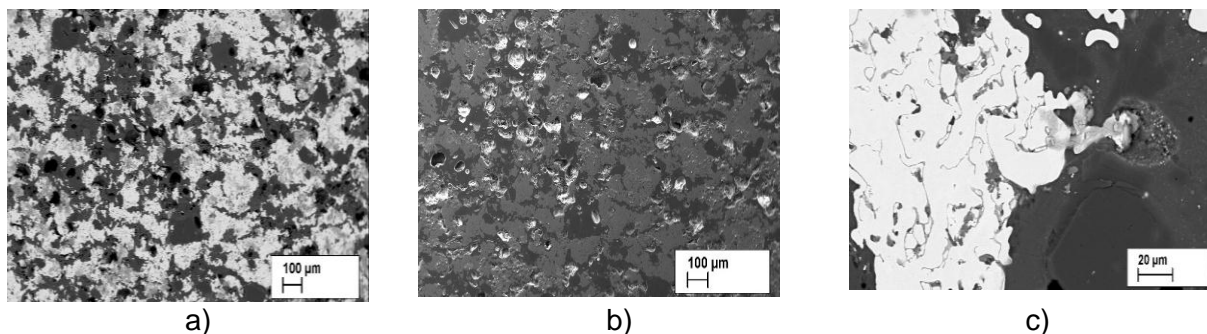


Figure.3 SEM images of obtained composite material with magnification a) X 50, BSE mode, b) X 50, SE mode, c) X500 BSE mode.

Table 3. EDX element analysis in atomic%.

Nr.	Composition in atomic%								
	O	Na	Mg	Al	Si	K	Ca	Ti	Fe
1	63,36	2,65	0,55	7,89	22,21	1,10	1,45	0,29	0,50
2	62,86	1,19	0,24	17,60	15,62	1,03	0,27	0,12	1,06
3	66,66	0,03	0,03	0,02	33,09	0,01	0,00	0,00	0,20
4	66,64	0,04	0,01	0,04	33,22	-0,02	0,01	0,01	0,19
5	4,40	0,28	0,02	0,09	0,08	0,02	0,06	-0,04	95,13
6	4,37	0,35	0,14	0,11	-0,08	-0,06	0,11	0,04	95,30
7	64,14	2,11	0,78	6,89	23,17	1,96	0,35	0,21	0,40

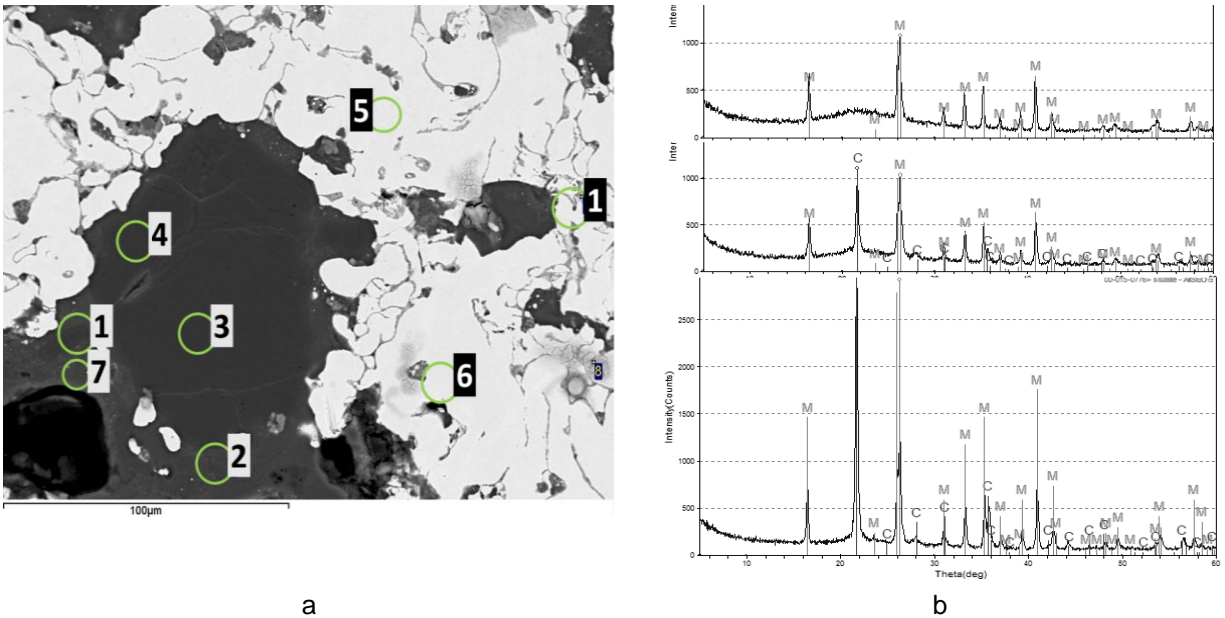


Figure.4 a) SEM image with magnification X 800 with EDX element analysis. b) X-ray diffractogramme of CS, from above downwards: raw material; sample heat treated at 1100°C; sample heat treated at 1200°C. Designations: C – cristobalite SiO_2 ; M – mullite $\text{Al}_6\text{Si}_2\text{O}_{13}$

3.2 Effect of CS on phase change.

The XRD patterns of CS sample were displayed in Fig. 4b. The thermal treated CS samples were composed of cristobalite, mullite and amorphous glass phase. But untreated CS consists of mullite and amorphous glass phase only. During sintering the cristobalite phase appear and crystallite size of cristobalite and mullite are growing up with sintering temperature increasing.

3.3. Apparent density and compression test

The density and compression strength of samples sintered at different temperatures was shown in Fig. 5. As can be seen from Fig. 5, the compression strength increased as the sintering temperature raised from 1100°C to 1200°C, which resulted from the clay and iron particles sintering. The apparent density firstly increased and then decreased as sintering temperature increased from 1150 to 1200°C. Apparent density reached its highest value when the samples were sintered at 1150°C.

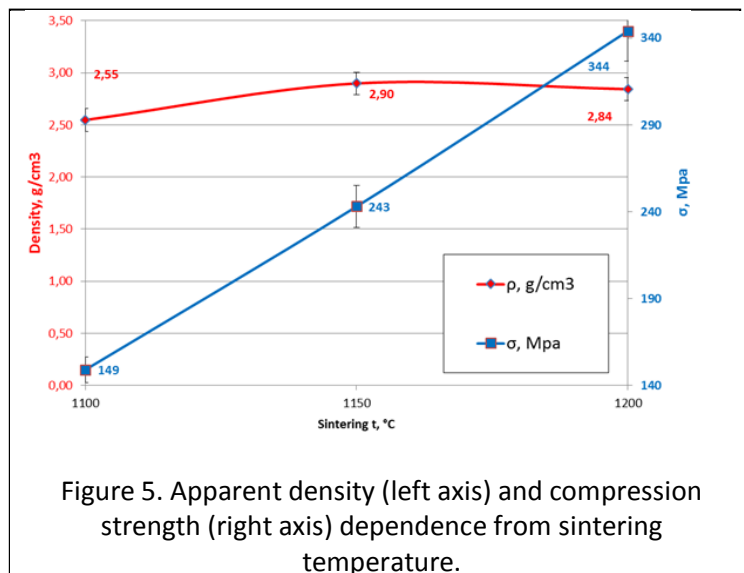


Figure 5. Apparent density (left axis) and compression strength (right axis) dependence from sintering temperature.

4. CONCLUSIONS.

1. Metal powder/fly ash cenosphere/modified clay, composite, with a density of 2.55-2.84 g/cm³ and compression strength of 149-344 MPa, were prepared by using fly ash cenospheres as density-decreasing agent clay as inorganic binder and iron powder as strengthening framework by semi-dry powder compaction route.

2. The compression strength of the obtained composite increases linearly as the sintering temperature increase while the density shows a maximum ($2.90\pm 0.03 \text{ g/cm}^3$) at a sintering temperature of 1150°C .
3. The compression strength shows a linear relationship with sintering temperature over the range $1100\text{-}1200^\circ\text{C}$.

BIBLIOGRAPHY

- [1] G. Stephani and M. Scheffler, "Cellular Materials - CELLMAT 2012," 2012. [Online]. Available: <http://www.conventus.de/cellmat/>. [Accessed: 27-Jan-2013].
- [2] J. Pang, Q. Li, W. Wang, X. Xu, and J. Zhai, "Preparation and characterization of electroless Ni-Co-P ternary alloy on fly ash cenospheres," *Surf. Coatings Technol.*, vol. 205, no. 17–18, pp. 4237–4242, May 2011.
- [3] F. Blanco, P. García, P. Mateos, and J. Ayala, "Characteristics and properties of lightweight concrete manufactured with cenospheres," *Cem. Concr. Res.*, vol. 30, no. 11, pp. 1715–1722, Nov. 2000.
- [4] N. Barbare, A. Shukla, and A. Bose, "Uptake and loss of water in a cenosphere-concrete composite material," *Cem. Concr. Res.*, vol. 33, no. 10, pp. 1681–1686, Oct. 2003.
- [5] J.-Y. Wang, M.-H. Zhang, W. Li, K.-S. Chia, and R. J. Y. Liew, "Stability of cenospheres in lightweight cement composites in terms of alkali-silica reaction," *Cem. Concr. Res.*, vol. 42, no. 5, pp. 721–727, May 2012.
- [6] Y. Shao, D. Jia, Y. Zhou, and B. Liu, "Novel Method for Fabrication of Silicon Nitride/Silicon Oxynitride Composite Ceramic Foams Using Fly Ash Cenosphere as a Pore-Forming Agent," *J. Am. Ceram. Soc.*, vol. 91, no. 11, pp. 3781–3785, Nov. 2008.
- [7] C. Wang, J. Liu, H. Du, and A. Guo, "Effect of fly ash cenospheres on the microstructure and properties of silica-based composites," *Ceram. Int.*, vol. 38, no. 5, pp. 4395–4400, Jul. 2012.
- [8] G. L. M. Li, J. P. Watson, and M. M. Bryant, "Effect of Cenospheres on Flyash Brick Properties," 2007.
- [9] T. a. Vereshchagina, S. N. Vereshchagin, N. N. Shishkina, N. G. Vasilieva, L. a. Solovyov, and A. G. Anshits, "Microsphere zeolite materials derived from coal fly ash cenospheres as precursors to mineral-like aluminosilicate hosts for ^{135}Cs and ^{90}Sr ," *J. Nucl. Mater.*, vol. 437, no. 1–3, pp. 11–18, Jun. 2013.
- [10] H. Qian, X. Cheng, H. Zhang, R. Zhang, and Y. Wang, "Preparation of Porous Mullite Ceramics Using Fly Ash Cenosphere as a Pore-Forming Agent by Gelcasting Process," *Int. J. Appl. Ceram. Technol.*, vol. 6, p. n/a–n/a, Dec. 2013.
- [11] A. A. Johnson, K. Mukherjee, S. Schlosser, and E. Raask, "The behaviour of a cenosphere-resin composite under hydrostatic pressure," *Ocean Eng.*, vol. 2, no. 1, pp. 45–48, Sep. 1970.
- [12] N. Chand, P. Sharma, and M. Fahim, "Correlation of mechanical and tribological properties of organosilane modified cenosphere filled high density polyethylene," *Mater. Sci. Eng. A*, vol. 527, no. 21–22, pp. 5873–5878, Aug. 2010.
- [13] A. Tiwari, H. S. Jaggi, R. K. Kachhap, B. K. Satapathy, S. N. Maiti, and B. S. Tomar, "Comparative performance assessment of cenosphere and barium sulphate based friction composites," *Wear*, vol. 309, no. 1–2, pp. 259–268, Jan. 2014.
- [14] "Mechanical and thermal characteristics of high density polyethylene-fly cenosphere composites.pdf."
- [15] M. Kulkarni, V. Bambole, and P. Mahanwar, "Effect of particle size of fly ash cenospheres on the properties of acrylonitrile butadiene styrene-filled composites," *J. Thermoplast. Compos. Mater.*, vol. 27, no. 2, pp. 251–267, May 2012.
- [16] N. Jha, A. Badkul, D. P. Mondal, S. Das, and M. Singh, "Sliding wear behaviour of aluminum syntactic foam: A comparison with Al-10wt% SiC composites," *Tribol. Int.*, vol. 44, no. 3, pp. 220–231, Mar. 2011.
- [17] Z. Y. Dou, L. T. Jiang, G. H. Wu, Q. Zhang, Z. Y. Xiu, and G. Q. Chen, "High strain rate compression of cenosphere-pure aluminum syntactic foams," *Scr. Mater.*, vol. 57, no. 10, pp. 945–948, Nov. 2007.
- [18] P. Rohatgi, N. Gupta, B. Schultz, and D. Luong, "The synthesis, compressive properties, and applications of metal matrix syntactic foams," *JOM*, vol. 63, no. 2, pp. 36–42, 2011.
- [19] D. P. Mondal, S. Das, N. Ramakrishnan, and K. Uday Bhasker, "Cenosphere filled aluminum syntactic foam made through stir-casting technique," *Compos. Part A Appl. Sci. Manuf.*, vol. 40, no. 3, pp. 279–288, Mar. 2009.
- [20] A. Shishkin, "Latvian clay and alumina-silica hollowspheres use for ceramics obtain. (in latvian)," Riga Technical University, 2013.
- [21] D. D. Luong, O. M. Strbik, V. H. Hammond, N. Gupta, and K. Cho, "Development of high performance lightweight aluminum alloy/SiC hollow sphere syntactic foams and compressive characterization at quasi-static and high strain rates," *J. Alloys Compd.*, vol. 550, pp. 412–422, Feb. 2013.
- [22] D. P. Mondal, J. Datta Majumder, N. Jha, A. Badkul, S. Das, A. Patel, and G. Gupta, "Titanium-cenosphere syntactic foam made through powder metallurgy route," *Mater. Des.*, vol. 34, pp. 82–89, Feb. 2012.